Next generation Advanced Laser Fluorometry (ALF) for characterization of natural aquatic environments: new instruments

Alexander Chekalyuk[1*] and Mark Hafez[1]

[1]*Lamont Doherty Earth Observatory of Columbia University, 61 Route 9W, Palisades, NY 10964, USA*
[*]*chekaluk@ldeo.columbia.edu*

Abstract: The new optical design allows single- or multi-wavelength excitation of laser-stimulated emission (LSE), provides optimized LSE optical collection for spectral and temporal analyses, and incorporates swappable modules for flow-through and small-volume sample measurements. The basic instrument configuration uses 510 nm laser excitation for assessments of chlorophyll-a, phycobiliprotein pigments, variable fluorescence (F_v/F_m) and chromophoric dissolved organic matter (CDOM) in CDOM-rich waters. The three-laser instrument configuration (375, 405, and 510 nm excitation) provides additional Fv/Fm measurements with 405 nm excitation, CDOM assessments in a broad concentration range, and potential for spectral discrimination between oil and CDOM fluorescence. The new measurement protocols, analytical algorithms and examples of laboratory and field measurements are discussed.

OCIS codes: (010.4450) Oceanic optics; (280.4788) Optical sensing and sensors; (300.0300) Spectroscopy; (140.0140) Lasers and laser optics.

References and links

1. A. M. Chekalyuk and M. Hafez, "Photo-physiological variability in phytoplankton chlorophyll fluorescence and assessment of chlorophyll concentration," Opt. Express **19**(23), 22643–22658 (2011).
2. A. M. Chekalyuk, M. Landry, R. Goericke, A. G. Taylor, and M. Hafez, "Laser fluorescence analysis of phytoplankton across a frontal zone in the California Current ecosystem," J. Plankton Res. **34**(9), 761–777 (2012).
3. Y. Dandonneau and J. Neveux, "Diel variations of in vivo fluorescence in the eastern equatorial Pacific: an unvarying pattern," Deep Sea Res. Part II Top. Stud. Oceanogr. **44**(9-10), 1869–1880 (1997).
4. P. Falkowski and D. A. Kiefer, "Chlorophyll-a fluorescence in phytoplankton - relationship to photosynthesis and biomass," J. Plankton Res. **7**(5), 715–731 (1985).
5. C. W. Proctor and C. S. Roesler, "New insights on obtaining phytoplankton concentration and composition from in situ multispectral chlorophyll fluorescence," Limnol. Oceanogr. Methods **8**, 695–708 (2010).
6. C. D. Wirick, "Exchange of phytoplankton across the continental shelf-slope boundary of the Middle Atlantic Bight during spring 1988," Deep Sea Res. Part II Top. Stud. Oceanogr. **41**(2-3), 391–410 (1994).
7. Y. Z. Yacobi, "From Tswett to identified flying objects: A concise history of chlorophyll a use for quantification of phytoplankton," Isr. J. Plant Sci. **60**(1), 243–251 (2012).
8. M. Beutler, K. H. Wiltshire, B. Meyer, C. Moldaenke, C. Lüring, M. Meyerhöfer, U. P. Hansen, and H. Dau, "A fluorometric method for the differentiation of algal populations in vivo and in situ," Photosynth. Res. **72**(1), 39–53 (2002).
9. A. M. Chekalyuk and M. Hafez, "Advanced laser fluorometry of natural aquatic environments," Limnol. Oceanogr. Methods **6**, 591–609 (2008).
10. T. J. Cowles, R. A. Desiderio, and S. Neuer, "In situ characterization of phytoplankton from vertical profiles of fluorescence emission spectra," Mar. Biol. **115**(2), 217–222 (1993).
11. H. L. MacIntyre, E. Lawrenz, and T. L. Richardson, "Taxonomic discrimination of phytoplankton by spectral fluorescence," in *Chlorophyll: A Fluorescence in Aquatic Sciences: Methods and Applications,* D. J. Suggett, O. Prasil, and M. A. Borowitzka, eds. (Springer, 2010).
12. P. B. Oldham and I. M. Warner, "Analysis of natural phytoplankton populations by pattern recognition of two dimensional fluorescence spectra," Spectrosc. Lett. **20**(5), 391–413 (1987).
13. G. Parésys, C. Rigart, B. Rousseau, A. W. M. Wong, F. Fan, J. P. Barbier, and J. Lavaud, "Quantitative and qualitative evaluation of phytoplankton communities by trichromatic chlorophyll fluorescence excitation with

#189252 - $15.00 USD Received 23 Apr 2013; revised 23 May 2013; accepted 24 May 2013; published 7 Jun 2013

special focus on cyanobacteria," Water Res. **39**(5), 911–921 (2005).
14. T. L. Richardson, E. Lawrenz, J. L. Pinckney, R. C. Guajardo, E. A. Walker, H. W. Paerl, and H. L. MacIntyre, "Spectral fluorometric characterization of phytoplankton community composition using the Algae Online Analyser," Water Res. **44**(8), 2461–2472 (2010).
15. J. Seppälä and M. Balode, "The use of spectral fluorescence methods to detect changes in the phytoplankton community," Hydrobiologia **363**(1/3), 207–217 (1997).
16. C. S. Yentsch and C. M. Yentsch, "Fluorescence spectral signatures characterization of phytoplankton populations by the use of excitation and emission spectra," J. Mar. Res. **37**, 471–483 (1979).
17. T. S. Bibby, M. Y. Gorbunov, K. W. Wyman, and P. G. Falkowski, "Photosynthetic community responses to upwelling in mesoscale eddies in the subtropical North Atlantic and Pacific Oceans," Deep Sea Res. Part II Top. Stud. Oceanogr. **55**(10-13), 1310–1320 (2008).
18. A. M. Chekalyuk, F. E. Hoge, C. W. Wright, and R. N. Swift, "Short-pulse pump-and-probe technique for airborne laser assessment of Photosystem II photochemical characteristics," Photosynth. Res. **66**(1/2), 33–44 (2000).
19. P. G. Falkowski and Z. Kolber, "Variations in chlorophyll fluorescence yields in phytoplankton in the world oceans," Aust. J. Plant Physiol. **22**(2), 341–355 (1995).
20. Z. Kolber and P. G. Falkowski, "Use of active fluorescence to estimate phytoplankton photosynthesis in situ," Limnol. Oceanogr. **38**(8), 1646–1665 (1993).
21. Z. S. Kolber, O. Prasil, and P. G. Falkowski, "Measurements of variable chlorophyll fluorescence using fast repetition rate techniques: defining methodology and experimental protocols," Biochim. Biophys. Acta **1367**(1-3), 88–106 (1998).
22. R. J. Olson, A. M. Chekalyuk, and H. M. Sosik, "Phytoplankton photosynthetic characteristics from fluorescence induction assays of individual cells," Limnol. Oceanogr. **41**(6), 1253–1263 (1996).
23. R. J. Olson, H. M. Sosik, and A. M. Chekalyuk, "Photosynthetic characteristics of marine phytoplankton from pump-during-probe fluorometry of individual cells at sea," Cytometry **37**(1), 1–13 (1999).
24. U. Schreiber, C. Neubauer, and U. Schliwa, "PAM fluorometer based on medium-frequency pulsed Xe-flash measuring light: a highly sensitive new tool in basic and applied photosynthesis research," Photosynth. Res. **36**(1), 65–72 (1993).
25. U. Schreiber, C. Klughammer, and J. Kolbowski, "Assessment of wavelength-dependent parameters of photosynthetic electron transport with a new type of multi-color PAM chlorophyll fluorometer," Photosynth. Res. **113**(1-3), 127–144 (2012).
26. C. E. Del Castillo, P. G. Coble, R. N. Conmy, F. E. Muller-Karger, L. Vanderbloemen, and G. A. Vargo, "Multispectral in situ measurements of organic matter and chlorophyll fluorescence in seawater: documenting the intrusion of the Mississippi River plume in the West Florida Shelf," Limnol. Oceanogr. **46**(7), 1836–1843 (2001).
27. N. Hudson, A. Baker, and D. Reynolds, "Fluorescence analysis of dissolved organic matter in natural, waste and polluted waters – a review," River Res. Appl. **23**(6), 631–649 (2007).
28. C. E. Brown and M. F. Fingas, "Review of the development of laser fluorosensors for oil spill application," Mar. Pollut. Bull. **47**(9-12), 477–484 (2003).
29. Q. Q. Liu, C. Y. Wang, X. F. Shi, W. D. Li, X. N. Luan, S. L. Hou, J. L. Zhang, and R. E. Zheng, "Identification of spill oil species based on low concentration synchronous fluorescence spectra and RBF neural network," Spectrosc. Spect. Anal. **32**(4), 1012–1015 (2012).
30. A. G. Ryder, T. J. Glynn, M. Feely, and A. J. G. Barwise, "Characterization of crude oils using fluorescence lifetime data," Spectrochim. Acta A Mol. Biomol. Spectrosc. **58**(5), 1025–1037 (2002).
31. R. J. Exton, W. M. Houghton, W. E. Esaias, R. C. Harriss, F. H. Farmer, and H. H. White, "Laboratory analysis of techniques for remote sensing of estuarine parameters using laser excitation," Appl. Opt. **22**(1), 54–64 (1983).
32. R. J. Exton, W. M. Houghton, W. Esaias, R. C. Haas, and D. Hayward, "Spectral differences and temporal stability of phycoerythrin fluorescence in estuarine and coastal waters due to the domination of labile cryptophytes and stabile cyanibacteria," Limnol. Oceanogr. **28**(6), 1225–1231 (1983).
33. L. Poryvkina, S. Babichenko, S. Kaitala, H. Kuosa, and A. Shalapjonok, "Spectral fluorescence signatures in the characterization of phytoplankton community composition," J. Plankton Res. **16**(10), 1315–1327 (1994).
34. S. Babichenko, L. Poryvkina, V. Arikese, S. Kaitala, and H. Kuosa, "Remote sensing of phytoplankton using laser induced fluorescence," Remote Sens. Environ. **45**(1), 43–50 (1993).
35. A. M. Chekalyuk, A. A. Demidov, V. V. Fadeev, and M. Y. Gorbunov, "Lidar monitoring of phytoplankton and organic matter in the inner seas of Europe-EARSeL," Adv. Remote Sens. **3**, 131–139 (1995).
36. F. E. Hoge and R. N. Swift, "Airborne simultaneous spectroscopic detection of laser-induced water Raman backscatter and fluorescence from chlorophyll a and other naturally occurring pigments," Appl. Opt. **20**(18), 3197–3205 (1981).
37. D. N. Klyshko and V. V. Fadeev, "Remote determination of concentration of impurities in water by the laser spectroscopy method with calibration by Raman scattering," Sov. Phys. Dokl. **23**, 55–59 (1978).
38. A. Andrade-Eiroa, M. Canle, and V. Cerda, "Environmental applications of excitation emission spectrofluorimetry: an in depth review I," Appl. Spectrosc. Rev. **48**(1), 1–49 (2013).
39. A. Andrade-Eiroa, M. Canle, and V. Cerda, "Environmental applications of excitation emission spectrofluorimetry: an in depth review II," Appl. Spectrosc. Rev. **48**(2), 77–141 (2013).
40. A. Nebbioso and A. Piccolo, "Molecular characterization of dissolved organic matter (DOM): a critical review,"

#189252 - $15.00 USD Received 23 Apr 2013; revised 23 May 2013; accepted 24 May 2013; published 7 Jun 2013

Anal. Bioanal. Chem. **405**(1), 109–124 (2013).
41. Z. Z. Zhou and L. D. Guo, "Evolution of the optical properties of seawater influenced by the Deepwater Horizon oil spill in the Gulf of Mexico," Environ. Res. Lett. **7**(2), 025301 (2012), doi:10.1088/1748-9326/7/2/025301.
42. Z. Z. Zhou, L. D. Guo, A. M. Shiller, S. E. Lohrenz, V. L. Asper, and C. L. Osburn, "Characterization of oil components from the Deepwater Horizon oil spill in the Gulf of Mexico using fluorescence EEM and PARAFAC techniques," Mar. Chem. **148**, 10–21 (2013).
43. Z. Z. Zhou, Z. F. Liu, and L. D. Guo, "Chemical evolution of Macondo crude oil during laboratory degradation as characterized by fluorescence EEMs and hydrocarbon composition," Mar. Pollut. Bull. **66**(1-2), 164–175 (2013).
44. M. L. Nahorniak and K. S. Booksh, "Excitation-emission matrix fluorescence spectroscopy in conjunction with multiway analysis for PAH detection in complex matrices," Analyst (Lond.) **131**(12), 1308–1315 (2006).
45. R. E. Davis, M. D. Ohman, D. L. Rudnick, J. T. Sherman, and B. Hodges, "Glider surveillance of physics and biology in the southern California Current System," Limnol. Oceanogr. **53**(5_part_2), 2151–2168 (2008).
46. M. J. Perry, B. S. Sackmann, C. C. Eriksen, and C. M. Lee, "Seaglider observations of blooms and subsurface chlorophyll maxima off the Washington coast," Limnol. Oceanogr. **53**(5_part_2), 2169–2179 (2008).
47. X. G. Xing, H. Claustre, S. Blain, F. D'Ortenzio, D. Antoine, J. Ras, and C. Guinet, "Quenching correction for in vivo chlorophyll fluorescence acquired by autonomous platforms: a case study with instrumented elephant seals in the Kerguelen region (Southern Ocean)," Limnol. Oceanogr. Methods **10**, 483–495 (2012).
48. X. Yu, T. Dickey, J. Bellingham, D. Manov, and K. Streitlien, "The application of autonomous underwater vehicles for interdisciplinary measurements in Massachusetts and Cape Cod Bays," Cont. Shelf Res. **22**(15), 2225–2245 (2002).
49. R. Alexander, P. Gikuma-Njuru, and J. Imberger, "Identifying spatial structure in phytoplankton communities using multi-wavelength fluorescence spectral data and principal component analysis," Limnol. Oceanogr. Methods **10**, 402–415 (2012).
50. R. Alexander and J. Imberger, "Phytoplankton patchiness in Winam Gulf, Lake Victoria: a study using principal component analysis of in situ fluorescent excitation spectra," Freshw. Biol. **58**(2), 275–291 (2013).
51. A. Catherine, N. Escoffier, A. Belhocine, A. B. Nasri, S. Hamlaoui, C. Yéprémian, C. Bernard, and M. Troussellier, "On the use of the FluoroProbe®, a phytoplankton quantification method based on fluorescence excitation spectra for large-scale surveys of lakes and reservoirs," Water Res. **46**(6), 1771–1784 (2012).
52. M. J. Doubell, L. Seuront, J. R. Seymour, N. L. Patten, and J. G. Mitchell, "High resolution fluorometer for mapping microscale phytoplankton distributions," Appl. Environ. Microbiol. **72**(6), 4475–4478 (2006).
53. M. J. Doubell, H. Yamazaki, H. Li, and Y. Kokubu, "An advanced laser-based fluorescence microstructure profiler (TurboMAP-L) for measuring bio-physical coupling in aquatic systems," J. Plankton Res. **31**(12), 1441–1452 (2009).
54. S. G. H. Simis, Y. Huot, M. Babin, J. Seppälä, and L. Metsamaa, "Optimization of variable fluorescence measurements of phytoplankton communities with cyanobacteria," Photosynth. Res. **112**(1), 13–30 (2012).
55. R. Röttgers and B. P. Koch, "Spectroscopic detection of a ubiquitous dissolved pigment degradation product in subsurface waters of the global ocean," Biogeosciences **9**(7), 2585–2596 (2012).
56. J. J. Cullen and R. F. Davis, "The blank can make a big difference in oceanographic measurements," Limnol. Oceanogr. Bull. **12**, 29–35 (2003).
57. E. Fuchs, R. C. Zimmerman, and J. S. Jaffe, "The effect of elevated levels of phaeophytin in natural waters on variable fluorescence measured from phytoplankton," J. Plankton Res. **24**(11), 1221–1229 (2002).
58. S. R. Laney and R. M. Letelier, "Artifacts in measurements of chlorophyll fluorescence transients, with specific application to fast repetition rate fluorometry," Limnol. Oceanogr. Methods **6**, 40–50 (2008).
59. R. M. Cory, M. P. Miller, D. M. McKnight, J. J. Guerard, and P. L. Miller, "Effect of instrument-specific response on the analysis of fulvic acid fluorescence spectra," Limnol. Oceanogr. Methods **8**, 67–78 (2010).
60. G. H. Krause and E. Weis, "Chlorophyll fluorescence and photosynthesis - the basics," Annu. Rev. Plant Physiol. **42**(1), 313–349 (1991).
61. M. Raateoja, J. Seppala, and P. Ylostalo, "Fast repetition rate fluorometry is not applicable to studies of filamentous cyanobacteria from the Baltic Sea," Limnol. Oceanogr. **49**(4), 1006–1012 (2004).

1. Introduction

Measurements of optically stimulated emission in oceanic, coastal, estuarine and fresh waters can provide rich and useful information about aquatic fluorescence constituents, including photosynthesizing phytoplankton, chromophoric dissolved organic matter (CDOM; see a list of abbreviations in Table 1), oil and poly-aromatic hydrocarbons (PAHs). Such measurements can be conducted in a broad range of constituent concentrations for qualitative and quantitative analyses of natural aquatic environments. *In vivo* fluorescence of chlorophyll-a (Chl-a) and accessory phycobiliprotein (PBP) pigments is used as an index of Chl-a concentration and phytoplankton biomass (e.g., [1–7]). It can also provide structural [8–16] and photophysiological (e.g., [17–25]) characterization of phytoplankton communities. The

#189252 - $15.00 USD Received 23 Apr 2013; revised 23 May 2013; accepted 24 May 2013; published 7 Jun 2013

broadband fluorescence of CDOM and PAHs can be used for assessment and characterization of CDOM (e.g., [26,27]), oil and oil products (e.g., [28–30]), respectively.

The emission signatures of natural waters are complex and highly variable, being composed by the overlapped spectral bands of various fluorescence constituents and water Raman scattering [9,31–33]. The intensity of constituent-specific fluorescence depends on the constituent absorption in the spectral range of excitation, its fluorescence efficiency and concentration. The former can be used to optimize retrieving constituent-specific information from the emission signatures via selecting the excitation wavelength close to maximum of the constituent fluorescence excitation spectrum. The latter provides a basis for fluorescence assessments of constituent concentrations. To improve the accuracy of fluorescence concentration measurements, it is desirable to minimize a potential variability in the fluorescence efficiency associated with environmental factors or constituent functional state. This can be achieved by appropriate selection of the measurement protocol (e.g., [1]). On the other hand, the variability in *in vivo* Chl-a fluorescence can be stimulated using various active fluorescence techniques to retrieve valuable information about phytoplankton photo-physiology and photochemical efficiency (see references above).

Table 1. Abbreviations used in text

Abbreviation	Term
A	Input aperture of an optical sensor
ALF	Advanced Laser Fluorometry/Fluorometer (method/instrument)
B_{NC}	The value of non-chlorophyll fluorescence background
BR	LSE back reflection
C	Measurement cell
CDOM	Chromophoric dissolved organic matter
Chl-a	Chlorophyll a (pigment)
C_{chl}	Chl-a concentration, μg L^{-1}
ECF_1, ECF_2	Emission collection-filtration optical units
F_1, F_2	Interference filter
FG	Optical fiber guide
F_v/F_m	Variable fluorescence
K_{SC}	Spectrometer spectral response
L_{C1}, L_{C2}	Lens used for LSE collection and collimation
L_{F1}, L_{F2}	Lens used for LSE focusing
LSE	Laser-stimulated emission
M_1	100% reflection mirror
M_2, M_3	45-degree dichroic mirrors
N	Number of data points involved in the correlation analysis
PAHs	Poly-aromatic hydrocarbons
PBP	Phycobiliprotein (pigments)
PDP	Pump-during-probe (measurement protocol [9,22])
PE	Phycoerythrin (pigment)
PMT	Photomultiplier
S1, S2	Spectrum in Fig. 3(a)
S_1, S_2, S_3	Laser excitation sources
SDC	Spectral deconvolution (method, technique [9])
W	Optical window

The spectral characteristics and intensity of water Raman scattering strongly depend on the spectral range of excitation [9]. Generally, the Raman band intensity is comparable to the fluorescence intensities of aquatic constituents in natural waters and often spectrally overlap with the fluorescence bands [9,34,35]. Therefore, the Raman scattering has to be accounted for when analyzing the measurements of stimulated emission. It can also be used to normalize the constituent fluorescence to adjust for variability in optical properties of natural waters and improve the constituent concentration assessments [36,37].

Laboratory benchtop scanning fluorometers are capable of spectrally tunable excitation and emission measurements, and allow detailed characterization of natural aquatic environments based on the fluorescence excitation-emission matrix measurements. Such

#189252 - $15.00 USD Received 23 Apr 2013; revised 23 May 2013; accepted 24 May 2013; published 7 Jun 2013

instruments are broadly used in environmental applications [38,39], for characterization of CDOM [40], phytoplankton [33], oil and oil products (e.g., [41–43]). On the other hand, such instruments are too bulky and heavy for their routine use in the field; the measurement scans take relatively long time, which makes high volume sample measurements impractical. The scanning fluorometers cannot be used for *in situ* and flow-through measurements, are not sensitive enough to measure the weak fluorescence signatures typical for marine and oceanic environments, and do not provide active fluorescence assessment of phytoplankton photo-physiological characteristics. Only a few relatively portable, custom-built fluorometers capable of the advanced excitation-emission analysis in the field have been developed (e.g., [12,44]).

The available field fluorometers overcome most of these limitations: they are compact, capable of fast and sensitive *in situ* or flow-through measurements, and can be deployed on various platforms, including autonomous unmanned vehicles, gliders, and animals (e.g., [45–48]). The past decade has resulted in development of several new instruments that extended analytical capabilities of the field fluorometry. In particular, a novel pulse amplitude modulation fluorometer provides multi-color fluorescence excitation and actinic illumination for improved photo-physiological assessments of phytoplankton [25]. A new fluorescence induction and relaxation instrument can be used for detailed characterization of phytoplankton photochemical parameters in the field [17]. The FluoroProbe instrument provides potential for basic structural characterization of phytoplankton community [8], though its analytical algorithms may need some adjustments with regard to specifics of diverse aquatic environments [14,49–51]. New microstructure profiling fluorometers have been recently developed for high resolution measurements of vertical distributions of phytoplankton in the euphotic layer [52,53].

Most of these field instruments are designed to measure one specific parameter (e.g., Chl-a, CDOM, oil, or variable fluorescence) and do not provide information about other fluorescent constituents for more comprehensive characterization of aquatic environments. Technically, these fluorometers are built on the assumption that the emission intensity in the spectral area of fluorescence band of interest represents the intensity of this band (i.e., there is no emission of other fluorescence constituents that can contribute in the spectral range of detection). Such assumption simplifies the instrument design and data interpretation: the measurements can be conducted via an appropriate band-pass filter using a compact and affordable photodetector, and the measured signal is solely attributed to the fluorescent constituent of interest.

Despite the attractiveness of this approach, the validity of such assumption needs evaluation on the case-by-case basis. As shown by various studies (e.g., [9,31–33,54]), it generally does not hold in the optically complex aquatic environments. Regardless of the spectral ranges of excitation and emission detection, the stimulated emission is often composed by the overlapped contributions of several spectral bands (for examples, see [9]). In particular, the broadband CDOM fluorescence can provide background spectral contribution comparable to the intensities of other spectral bands in the UV and visible portions of the emission spectra. This has to be accounted for when analyzing measurements of oil, PAHs, PBPs, and Chl fluorescence. The CDOM background may be comparable and even exceed the intensity of phycoerythrin (PE) fluorescence in the orange portion of emission spectrum (for examples, see Section 5). The so called “red stuff” fluorescence, which presumably originates from the accessory pigments of partially dysfunctional photosynthetic apparatus of phytoplankton, as well as phycocyanin and allophycocyanin fluorescence can provide substantial contributions in the spectral area of Chl-a fluorescence ([9,55], see Section 5.1 for example). The spectral overlap may not only affect the accuracy of fluorescence concentration measurements, but also the photo-physiological assessments ([9,54,56–58]; see Section 5 for example and discussion).

#189252 - $15.00 USD Received 23 Apr 2013; revised 23 May 2013; accepted 24 May 2013; published 7 Jun 2013

The Advanced Laser Fluorometry (ALF) is an analytical technique that has been recently developed to address the optical complexity of natural aquatic environments and provide characterization of the key fluorescence constituents [9]. It provides *in vivo* fluorescence assessments of phytoplankton pigments, biomass, photophysiology, PBP-containing phytoplankton groups, and CDOM. The original ALF fluorometer is a compact flow-through instrument that combines spectral and temporal measurements of laser-stimulated emission (LSE) using dual-wavelength excitation at 405 and 532 nm. It can be used for underway shipboard measurements and analysis of discrete water samples. The spectral deconvolution (SDC) analysis of the LSE signatures was developed to assess the overlapped spectral bands of aquatic fluorescence constituents. Along with the accurate concentration measurements, the SDC analysis provides quantification of the non-chlorophyll fluorescence background in the spectral area of Chl-a fluorescence for more accurate phytoplankton photo-physiological assessments [9]. On the other hand, the ALF measurements of variable fluorescence can be used to improve measurements of Chl-a concentration [1].

In 2005-2011, the ALF technique was extensively tested in diverse water types, and proved to be a useful tool for aquatic research and environmental monitoring (e.g., [2]). Along with valuable observations, these field deployments helped to identify some design solutions, measurement and analytical protocols that can be further refined. The recent technological progress has resulted in availability of new optical components, including miniature lasers with new emission wavelengths. These factors have facilitated developing the next generation ALF technology and analytical algorithms reported in this article.

We describe a new ALF-T instrument that provides two-fold increase in the LSE collection efficiency in the analyzed spectral range. A new 510 nm laser module is used in the basic instrument configuration for spectral and temporal LSE measurements. The new compact "T" optical design is expandable to accommodate several excitation lasers. It provides easy access to the measurement compartment and incorporates swappable sampling modules for various applications. The new robust rail mounting system eliminates the need in alignment of optical components. Both single-laser and three-laser instrument configurations are described. The latter includes 375, 405, and 510 nm lasers and provides potential for detection of oil fluorescence and its spectral discrimination from the background CDOM fluorescence along with the basic ALF analytical capabilities described in [9]. The ALF-T analytical algorithms include real-time correction for the instrument spectral response and a new set of instrument-independent spectral components that can be used for SDC analysis of emission spectra measured with other spectrofluorometers. Examples of laboratory and field measurements illustrate the analytical capabilities of the ALF-T technique.

2. ALF-T instrument

2.1 Optical design

A block diagram of the ALF-T instrument is displayed in Fig. 1. The ALF-T optical design builds upon the "T" optical scheme optimized to provide efficient excitation and LSE collection from a liquid sample. It provides up to four-fold overall LSE increase vs. a conventional 90-degree optical scheme. One or several laser modules ($\mathbf{S_1}$, $\mathbf{S_2}$ and $\mathbf{S_3}$ in Fig. 1) can be used to stimulate the emission from the water sample in cell **C**. The 45-degree dichroic mirrors $\mathbf{M_2}$ and $\mathbf{M_3}$ direct the excitation beams from lasers $\mathbf{S_2}$ and $\mathbf{S_3}$ along the main excitation axis (**1**). A 100% mirror $\mathbf{M_1}$ reflects the laser beam/s (**1'**) back into the sample cell **C** to double the excitation intensity in optically-thin sample.

The "T" optical configuration includes two emission collection-filtration optical units, $\mathbf{ECF_1}$ and $\mathbf{ECF_2}$ (Fig. 1). An LSE portion (**2**) emitted from C towards $\mathbf{ECF_1}$ is collected and collimated (**3**) by lens $\mathbf{L_{C1}}$, filtered (**4**) by interference filter $\mathbf{F_1}$ to reduce the amount of elastic scattering of excitation in the LSE, and focused (**5**) by lens $\mathbf{L_{F1}}$ onto the input aperture **A** of an optical sensor associated with $\mathbf{ECF_1}$ (optionally, **A** can be an input aperture of a fiber **FG**

#189252 - $15.00 USD Received 23 Apr 2013; revised 23 May 2013; accepted 24 May 2013; published 7 Jun 2013

guiding the LSE to the sensor). An LSE portion (**2'**) emitted from **C** towards $\mathbf{ECF_2}$ is collected and collimated (**3′**) by lens $\mathbf{L_{C2}}$, filtered (**4'**) by interference filter $\mathbf{F_2}$, and focused (**5′**) by lens $\mathbf{L_{F2}}$ onto the input aperture of the $\mathbf{ECF_2}$ optical sensor (or a fiber guiding the collected LSE to the sensor).

A quality interference filter can reflect a significant amount of emission in the spectral range outside the filter transparency. The "T" optical scheme is designed to direct this reflected emission for analysis by the sensor associated with the ECF unit located in the opposite shoulder of the "T" scheme. In particular, the interference filter $\mathbf{F_2}$ reflects an LSE portion (3′) in a broad spectral range outside its transparency band. The reflected emission is focused by $\mathbf{L_{C2}}$ into **C**, passes it, and follows the optical path of LSE portion (**2**), which is directly emitted from **C** towards $\mathbf{ECF_1}$ (i.e. it is collected and collimated by $\mathbf{L_{C1}}$, filtered by $\mathbf{F_1}$, and can be focused after the filtration onto **A** by $\mathbf{L_{F1}}$).

Thus, a spectral portion of LSE initially emitted from the sample towards $\mathbf{ECF_2}$ can be delivered to the sensor associated with $\mathbf{ECF_1}$ in addition to the LSE directly emitted from the sample towards $\mathbf{ECF_1}$. This may provide substantial, about two-fold enhancement in the signal generated by the $\mathbf{ECF_1}$ sensor if at least a portion of the $\mathbf{F_2}$ spectral reflection range coincides with the $\mathbf{F_1}$ transmission band. Similarly, a spectral portion of (**3**), which is reflected (**3**```) by $\mathbf{F_1}$ towards **C**, may also result (after passing $\mathbf{L_{C1}}$, **C**, $\mathbf{L_{C2}}$, and $\mathbf{F_2}$) in up to two-fold increase in the LSE intensity reaching the $\mathbf{ECF_2}$ photosensor in the spectral range outside the $\mathbf{F_1}$ spectral transparency that matches the $\mathbf{F_2}$ transmission band.

Various instruments for spectral and/or temporal measurements of LSE from optically thin liquid or solid samples can be configured using the "T" optical design. For example, it can be used for optimizing concurrent measurements of laser-stimulated Stokes and anti-Stokes Raman scattering using appropriate long-pass ($\mathbf{F_1}$) and short-pass ($\mathbf{F_2}$) filters, respectively. Overall, it may provide up to four-fold increase in the intensity of both signals due to (i) doubling the excitation intensity caused by reflection of the excitation beam into the sample by $\mathbf{M_1}$ and (ii) doubling the intensity of the collected Stokes and anti-Stokes LSE signals due to their reflection by $\mathbf{F_1}$ and $\mathbf{F_2}$, respectively.

Here, we describe two instrument configurations for spectral characterization of fluorescence constituents in natural water samples and assessment of phytoplankton photochemical efficiency. The single-laser instrument, ALF-T-510 (Figs. 2(a) and 2(b)), employs a new 510 nm laser module (30 mW, model TECGL-30G-510, World Star Tech, Inc.) as an excitation source for spectral assaying of phytoplankton pigments and measurements of Chl-a fluorescence induction for phytoplankton photo-physiological assessments. Though the green excitation is not optimal for measuring CDOM fluorescence, it can be spectrally detected and discriminated vs. pigment fluorescence in CDOM-rich coastal, estuarine and fresh waters.

#189252 - $15.00 USD Received 23 Apr 2013; revised 23 May 2013; accepted 24 May 2013; published 7 Jun 2013

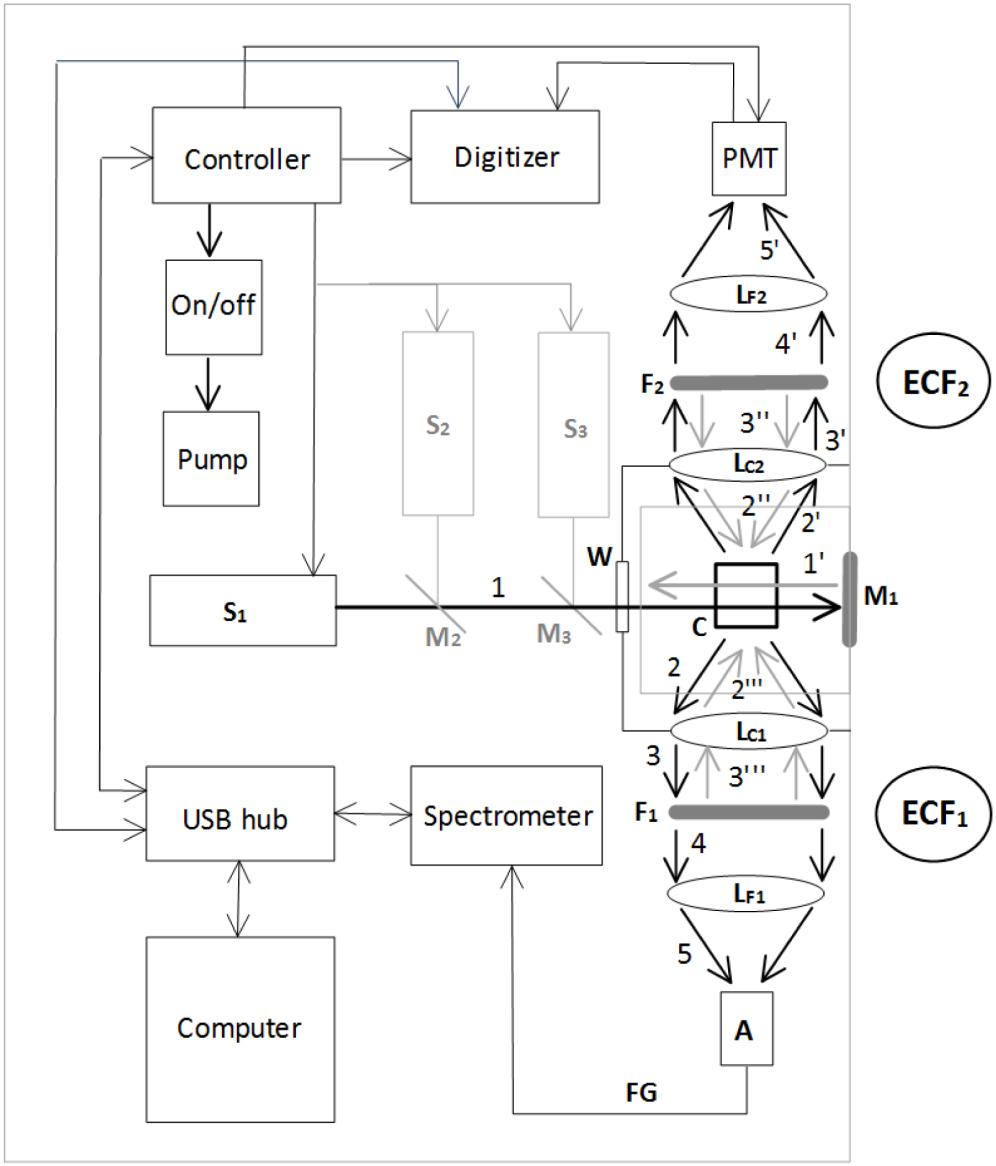

Fig. 1. Block diagram of the ALF-T instrument for spectrally and temporally resolved measurements of laser-stimulated emission in liquids. **ECF_1** and **ECF_2** are the emission collection-filtration units; (**C**) is a sample cell. The instrument design is described in detail in section 2.

#189252 - $15.00 USD Received 23 Apr 2013; revised 23 May 2013; accepted 24 May 2013; published 7 Jun 2013

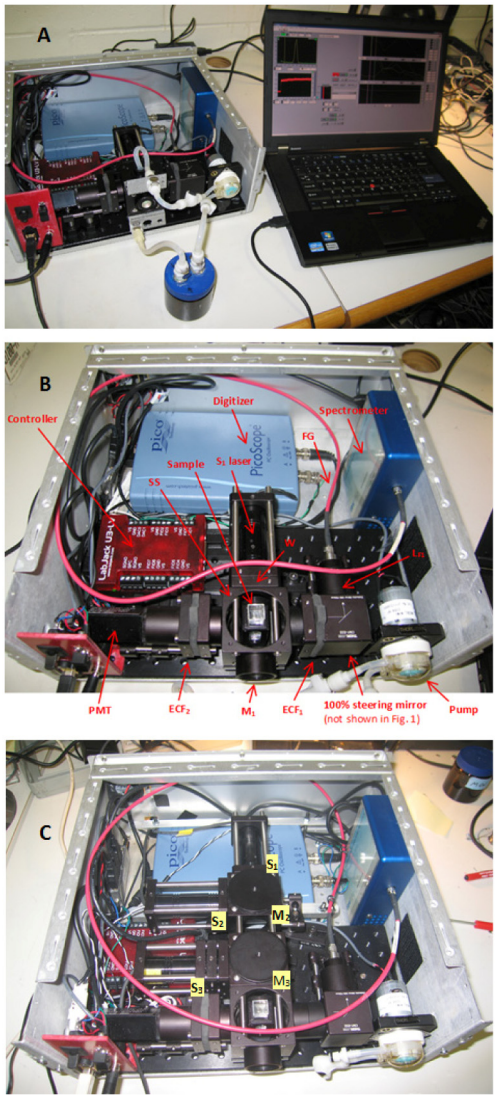

Fig. 2. Various configurations of the ALF-T instrument. **A:** The ALF-T-510 instrument configured for flow-through sample measurements. **B:** A close-up photo of the ALF-T-510 instrument configured for still sample measurements in the fluorometric cuvette. **C:** The ALF-T-375/405/510 instrument comprises three laser modules for LSE excitation at 375, 405, and 510 nm.

The three-laser instrument configuration, ALF-T-375/405/510 (Fig. 2(c)) includes 375, 405 and 510 nm lasers used as the excitation sources S_3, S_2 and S_1, respectively (Fig. 1) (models TECBL-100G-375-TTL (100 mW), TECBL-30G-405-TTL (30 mW), TECGL-30G-510 (30 mW), respectively; World Star Tech., Inc.). In addition to the ALF-T-510 analytical capabilities, it can be used for CDOM measurements in a very broad range of CDOM concentrations (including low-CDOM oligotrophic waters), as well as for detection of oil and PAHs. The ALF broadband high-resolution spectral measurements provide potential for discrimination of PAH spectral signatures vs. CDOM background fluorescence. The optical components used in the ALF-T-510 and ALF-T-375/405/510 instrument configurations are listed in Table 2. Thor Labs 30 mm cage mounting system used in the ALF-T optical design provides robustness, modular expandability, and eliminates a need in the optical alignment.

#189252 - $15.00 USD Received 23 Apr 2013; revised 23 May 2013; accepted 24 May 2013; published 7 Jun 2013

Table 2. Optical components (F1 and F1a,b are for ALF-T-510 and ALF-T-375/405/510 instruments, respectively).

Comp.	M_1	M_2	M_3	L_{C1}, L_{C2}	L_{F1}	L_{F2}	FG	F1	F1a	F1b	F2
Part #	BB1-E02	464DCLP	389DCLP	LA1805-A	LA1951-A	F810SMA-543	FH22-910	FF01-519/LP	BLP01-405R	ZX000277	FF01-684/24
Manufact.	Thor Labs	Omega	Omega	Thor Labs	Thor Labs	Thor Labs	Thor Labs	Semrock	Semrock	Iridian	Semrock

2.2 Electronics

The ALF-T electronic design (Fig. 1) includes several new components that improve instrument performance vs. the original ALF instrument [9] and enable more compact instrument design, thus providing potential for upgrading the instrument with additional laser excitation sources (e.g., Fig. 2(c)). A new small photomultiplier (PMT) module (H10721-20, Hamamatsu), which provides enhanced sensitivity in red spectral area of Chl-a fluorescence, and a 12-bit waveform digitizer (PS4224, PicoScope) with increased input sensitivity improve measurements of LSE fluorescence induction even at ultra-low, below 0.01 μg/L, Chl-a concentration. A compact spectrometer (Compass X, BWTek, Inc.) with thermoelectrically-cooled 2048-pixel CCD is used for spectral LSE measurements (Fig. 2(b)). The instrument operation is controlled via a small multifunctional USB board ("Controller"; model U3, LabJack Corporation) connected to the external rugged notebook computer (e.g., Toughbook T52, Panasonic) via a USB hub mounted inside the instrument case. A miniature peristaltic pump (WPM, WELCO Co, Ltd.) mounted on the front panel of the instrument case (Fig. 2(b)) is used for flow-through measurements of discrete water samples. The pump is controlled via a digital output of the USB controller board using a relay power switch (70M-ODC5, Grayhill). The laser excitation can be turned on/off via digital output of the USB controller connected to the TTL modulation pins of the laser modules. The PMT gain is adjusted in a broad range using analog output of the USB controller connected to the gain control of the PMT module. The ALF-T components are mounted in a compact, laptop footprint instrument case (Fig. 2) (ELMA Electronics, Inc.).

2.3 Sample compartment

The T-optical design provides easy access to the measurement area from the front panel of the instrument case (Figs. 1, 2) to simplify the measurements and instrument maintenance, and reduce the sample volume. The electronic and optical instrument components can be isolated from the sample compartment with an internal wall that has an optical window W (Fig. 1) transparent for the excitation to protect the optics and electronics from an accidental sample leak. The ALF-T instrument design incorporates swappable sampling modules to configure the instrument for various applications. Each module is assembled in a metal cube (C6W, Thor Labs) with the excitation reflection mirror M_1 (Figs. 1, 2). Optionally, this mirror can be substituted with a light source (e.g., LED) for sample illumination used in studies of phytoplankton photo-physiology (e.g., [2]). Four metal rods extended into the measurement area from the optical mounting system (Fig. 2) provide positioning and optical alignment of the sampling modules vs. instrument optical components. The current ALF-T configuration includes two sampling modules for flow-through measurements and analysis of small sample volumes. The flow-through module includes a glass flow cell (RF-1010-F, Spetrocell) that can be connected to the external source of liquid sample via silicon tubes (e.g., 14-176-332B,

#189252 - $15.00 USD Received 23 Apr 2013; revised 23 May 2013; accepted 24 May 2013; published 7 Jun 2013

Thermo Scientific Nalgene), water connectors (PMCD1602, Colder Products) and the instrument (or external) sampling pump. The flow-through module can be used for the shipboard underway measurements or analysis of discrete water samples from 100 to 500 ml glass bottles [1,9]. In the latter case, the intake sampling tube connects the sample bottle and the bottom input of the flow cell, while the top output of the flow cell is connected to the instrument peristaltic pump operating at 80 mL/min (Fig. 2(a)). The pump output can be connected to the sample bottle for sample circulation, or to a waste container if returning the sample exposed to the laser excitation is not desirable (for example when measuring fluorescence from dark-adapted phytoplankton ([1])). Standard 1x1x4 cm glass or disposable plastic fluorometric cells (e.g., A-108, Spectrocell; 14-955-130, Fisherbrand) can be used for measurements in the small sample module (Figs. 2(b) and 2(c)).

3. ALF-T measurements

3.1 ALF-T spectral and temporal measurements

The ALF-T measurements are conducted automatically, under control of the ALF-T operational software (developed using the LabView instrument control software; National Instruments). Various measurement protocols can be configured on the basis of ALF-T spectral and temporal LSE measurement capabilities.

The ALF-T spectral measurement sub-cycle includes turning on the laser excitation via the controller board, accumulation of the LSE spectrum by the CCD sensor of the spectrometer, turning off the laser, and transferring the measured LSE spectrum to the instrument computer via USB hub for storage, processing, analysis and display. The spectrometer operation is controlled by the instrument software via USB port. The spectral integration time is automatically adjusted depending on the LSE intensity and can range 0.1 to 3 s (depending on the excitation source and constituent concentration) to provide acceptable signal/noise ratio for quantitative assessments of fluorescence constituents.

The ALF-T temporal measurement sub-cycle begins with activating the controller board TTL pulse generator that triggers 250 μs laser excitation flashes repeating at 10-25 Hz and the waveform digitizer. The LSE induction in the spectral area of Chl-a fluorescence caused by the flash-induced saturation of photochemistry in photosystem II [9,22] is captured by the PMT module connected to the waveform digitizer and transferred via USB hub to the instrument computer. To improve the signal/noise ratio and better represent the sample volume, the ALF-T software averages the LSE waveforms over 5 to 100 flashes, depending on the LSE signal intensity. The PMT gain and input range of the waveform digitizer can be automatically adjusted to optimize the measurement regime with regard to the signal intensity.

3.2 ALF-T measurement protocols

The ALF-T instrument can be used for fluorescence measurements in various sampling modes and settings, including:

- flow-through monitoring of temporal variability in continuous water flow provided by external or internal sampling system (for example, shipboard underway measurements of horizontal variability of fluorescent constituents, or monitoring of temporal variability in stationary setting (e.g., pier, platform, or buoy);
- flow-through analysis of discrete water samples from sampling bottles;
- measurements of still water samples in standard fluorometric cell.

The ALF-T operation is optimized with regard to specifics of these measurements. During the flow-through measurements in the continuous water flow, each measurement cycle of the ALF-T-510 instrument consists of alternative sub-cycles of the spectral and temporal LSE measurements described above. The overall duration of the ALF-T-510 measurement cycle

#189252 - $15.00 USD Received 23 Apr 2013; revised 23 May 2013; accepted 24 May 2013; published 7 Jun 2013

may vary in a 1-10 second range, depending on the instrument settings. The spectral integration time, PMT gain, and input range of the waveform digitizer can be automatically adjusted with regard to the LSE signal variability. The measurement results are analyzed in real time, displayed on the computer monitor, and stored on the hard drive along with the measurement time and screen captures of informative portions of the user interface. During the shipboard underway measurements, the software can import the GPS data via serial interface to display the transect map and save the coordinates along with measurement data. Complementary data from shipboard sensors on seasurface temperature, salinity, oxygen and Chl-a can be also imported, displayed and stored along with the ALF-T fluorescence measurements.

The ALF-T-510 discrete sample analysis from the sampling bottles begins with automatic turning on the instrument pump to deliver the sample from the bottle into the flow cell. The pump remains on during the measurement cycle to ensure removal of the sample volume exposed to the excitation light from the measurement area to assay fluorescence characteristics of phytoplankton in their original photo-adapted state [1]. The measurements begin automatically, after several-second preset delay to ensure arrival of the sampled water into the excitation area. The sample analysis begins with the temporal measurements of Chl-a fluorescence induction. The LSE waveform is averaged over 50-100 excitation flashes and stored in the computer memory and on the hard drive. After measuring the LSE induction, several (5 to 15) LSE spectral measurements with 0.5-3 s integration time are automatically conducted to average the LSE spectrum over the sample volume and improve the signal/noise ratio. The sampling pump is turned off after the last spectral measurement. Data processing is completed after the measurement to maximize the amount of measurements during the sample run. The ALF-T analysis of the still water sample in the standard fluorometric cell is similar to the sample measurements from the bottles, except the instrument pump is not involved and the number of pump-during-probe (PDP) [9, 22] shots and spectral measurements is reduced to 15 and 7, respectively, to minimize the potential excitation-induced effect of non-photochemical quenching on the measurement results [1].

The default ALF-T-375/405/510 measurement cycle of the continuous flow-through measurements includes (i) spectral measurement with 375 nm laser, (ii) spectral and PDP measurement with 405 nm laser, and (iii) spectral and PDP measurement with 510 nm laser. The overall duration of the measurement cycle may vary in 10-25 s range, depending on the preset parameters of the spectral and temporal measurement sub-cycles. The ALF-T-375/405/510 discrete sample analysis begins with the fluorescence induction measurements using the 405 nm and 510 nm lasers. The LSE waveforms measured with 405 and 510 nm excitation are averaged over 50-100 excitation flashes. The temporal LSE measurements are followed by several (7-20, depending on the sample volume and measurement settings) alternate LSE spectral measurements with 375, 405, and 510 nm excitation. Such measurement protocol allows minimizing the potential effect of excitation-induced non-photochemical quenching on the photo-physiological assessments derived from the temporal LSE measurements [1]. The measurement cycle can be completed in 15-60 s, depending on the preset parameters of the spectral and temporal measurements involved.

4. Data processing and analysis

The ALF-T analytical algorithms include:

1. Correction of the LSE spectral measurements for instrument spectral response to yield the instrument-independent LSE spectral signatures
2. Spectral deconvolution (SDC) of the LSE to determine intensities of the overlapped spectral bands of aquatic fluorescent constituents

#189252 - $15.00 USD Received 23 Apr 2013; revised 23 May 2013; accepted 24 May 2013; published 7 Jun 2013

3. Calculation of fluorescence intensities normalized to the intensity of water Raman scattering also retrieved by the SDC analysis

4. Calculation of non-chlorophyll fluorescence background (B_{NC}) in the spectral area of Chl-a fluorescence, and B_{NC} subtraction from the PDP fluorescence induction curve

5. Best fitting to the spectrally-corrected for B_{NC} fluorescence induction curve with a biophysical model to determine photochemical efficiency of photosystem II (F_v/F_m, called "variable fluorescence").

Steps 2-5 are basically similar to the analytical algorithms that were earlier developed [9] and extensively tested in the field [1,2,9]. The major upgrades that we describe below include (i) the correction of LSE spectral measurements for the instrument spectral response and (ii) development of the new, instrument-independent SDC spectral components.

4.1 Correction for instrument spectral response

The instrument spectral response (i.e. wavelength dependence of spectrometer signal per LSE unit) is determined by the spectrometer sensor, optical filters and other components of the instrument. It may significantly vary in the measurement spectral range, resulting in the instrument dependence of spectral measurements. While useful information can be retrieved from the raw, instrument-dependent spectral measurements (e.g., [9]), eliminating dependence of the measured spectra on the instrument characteristics is often desirable (e.g., [59]), to allow relating with the measurements conducted using different instruments. We have incorporated the correction of ALF-T spectral measurements for the instrument spectral response and developed a new, instrument-independent set of spectral components. These components can be used for SDC analysis of any instrument-independent spectral data, including measurements with the ALF and commercial benchtop spectrofluorometers.

The ALF-T-510 spectral response between 540 and 750 nm, where the SDC procedure is conducted for the spectra measured with 510 nm excitation, is mainly determined by the spectrometer spectral response, and the spectrally-dependent LSE back reflection (BR) from the red bandpass interference filter $\mathbf{F_2}$ (Fig. 1). The spectrometer spectral response, $\mathbf{K_{SC}}$, was measured using a calibration lamp with a broadband spectral distribution (LS-1CAL, Ocean Optics), which was connected to the input slit of the spectrometer via 0.8 mm glass fiber (FH 22-910-CUSTOM, Thor Labs) that is also used in the ALF-T instrument to deliver the collected LSE to the input slit of the spectrometer (**FG** in Fig. 1). The $\mathbf{K_{SC}}$ array (blue dashed line in Fig. 3) was calculated via normalizing the measured lamp spectrum to the factory-calibrated spectral distribution of the lamp intensity.

To quantify the BR component of the spectral modulation, the broadband LSE spectrum of phytoplankton culture *Rhodomonas Sp* (cryptophyte) was measured with 510 nm laser excitation (i) using the ALF-T optical setup displayed in Fig. 1 (spectrum **S2** in Fig. 3(a)) and (ii) with the BR blocked by the black matte paper screen inserted between the measurement cell **C** and lens $\mathbf{L_{C2}}$ (spectrum **S1** in Fig. 3(a)). BR blocking has resulted in substantial, ~2-fold decrease in the signal intensity over most portion of the spectrum, except the red transmission band of filter $\mathbf{F_2}$ (marked with green vertical lines in Fig. 3(a)), where the signal intensities of Chl-a fluorescence peaks were identical in both spectra due to the low BR effect in spectrum **S2**. This illustrates that the LSE BR reflection incorporated in the ALF-T optical design indeed provides significance enhancement in the broad spectral range of the LSE signal analyzed by the spectrometer. It allows reducing the integration time to conduct faster or more frequent measurements, or using less powerful lasers to reduce the instrument cost, size, and power consumption. On the other hand, the LSE spectral measurements have to be corrected before the SDC analysis for the 2-fold decline ("red gap") in the LSE collection efficiency in the transparency band of the $\mathbf{F_2}$ filter. The **BR** array to correct for the "red gap" was derived from the spectral dependence of a ratio of **S2** and **S1** intensities, **S2/S1** (dark red line in Fig. 3(a)), smoothed using a "moving average" algorithm.

#189252 - $15.00 USD Received 23 Apr 2013; revised 23 May 2013; accepted 24 May 2013; published 7 Jun 2013

The automatic correction of the ALF-T spectral measurements for the instrument spectral response is conducted by the ALF-T software immediately after the measurements. It involves two steps as illustrated in Fig. 3(b) for the LSE seawater spectrum (black line)

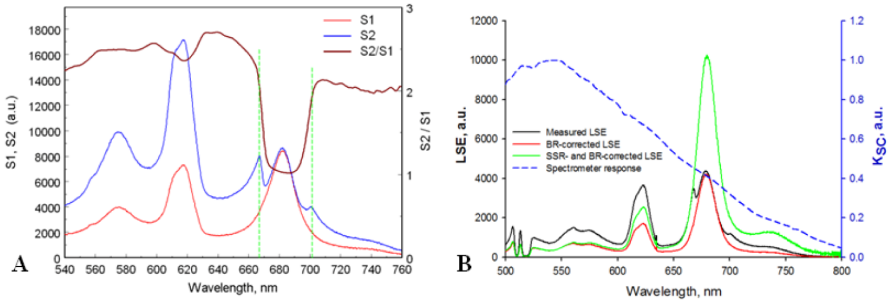

Fig. 3. **A:** Comparison of LSE spectral measurement (S2) using the ALF-T-514 instrument configuration (Fig. 2), and the LSE spectrum (S1) from the same sample when the LSE beams 2' and 2" were blocked. The ratio S2/S1 is used to correct to LSE spectral measurements for the "red gap" (667-703 nm) in the LSE back reflection. **B:** An example of two-step correction of the ALF-T spectral measurements for the instrument spectral response: (1) Normalizing the measured LSE spectrum (black) to the BR correction function (dark red line in panel (**A**) eliminates the modulation by the BR "red gap" (red line in panel (**B**). (2) Normalizing the BR-corrected spectrum (red) to the spectrometer spectral response yields the LSE spectrum corrected for the instrument spectral response (green).

measured with 510 nm excitation during a research cruise in the California Current (Aug. 2012). A drop in the spectral intensity around Chl-a fluorescence peak at 680 nm was caused by the "red gap" of the instrument spectral response (Fig. 3(a)) due to low LSE reflection of F_2 interference filter (Fig. 1) in its transparency range (665-700 nm). Normalizing the measured LSE spectrum to the BR correction array (dark red line in Fig. 3(a)) eliminates the "red gap" modulation (red line in Fig. 3(b)). The BR-corrected spectrum is then normalized to K_{SC} spectral distribution (blue dashed line in Fig. 3(b)) to correct it for the spectrometer spectral response. This results in the instrument-independent LSE spectrum (green line in Fig. 3(b)) that can be further analyzed using the SDC algorithm to retrieve the constituent-specific spectral components from the overlapped LSE spectral signature.

4.2 Spectral components for LSE spectral deconvolution (SDC) analysis

A new set of constituent-specific spectral components was developed for SDC analysis [9] of LSE spectra stimulated at four excitation wavelengths (375, 405, 510, and 532 nm) and corrected for the instrument spectral response. Along with 405 and 532 nm excitation used in the original ALF instrument, the ALF-T SDC component set includes new spectral components, specific for the new excitation wavelengths, 375 and 510 nm, that can be used to further extend the ALF analytical capabilities. The component development procedures were similar to those outlined in [9], but the LSE spectra used for the component development were corrected for the instrument spectral response as described in the previous section. Therefore, the new SDC components are instrument-independent and can be used for SDC analysis of aquatic emission spectra measured with any spectrofluorometer that provides correction for the instrument spectral response.

The new SDC spectral components are listed in Table 3. The list includes three components (elastic scattering (E_E), CDOM fluorescence (E_{CDOM}), and water Raman scattering (E_R)) with spectral characteristics dependent on the excitation wavelength. Four groups of such components are listed in the table for 375, 405, 510, and 532 nm excitation, respectively. In addition, Table 3 lists three groups of pigment fluorescence components that can be used for spectral discrimination and quantification of Chl-a, phycobiliprotein, and red fluorescence in the LSE spectra of natural waters [9]. Spectral characteristics of pigment

#189252 - $15.00 USD Received 23 Apr 2013; revised 23 May 2013; accepted 24 May 2013; published 7 Jun 2013

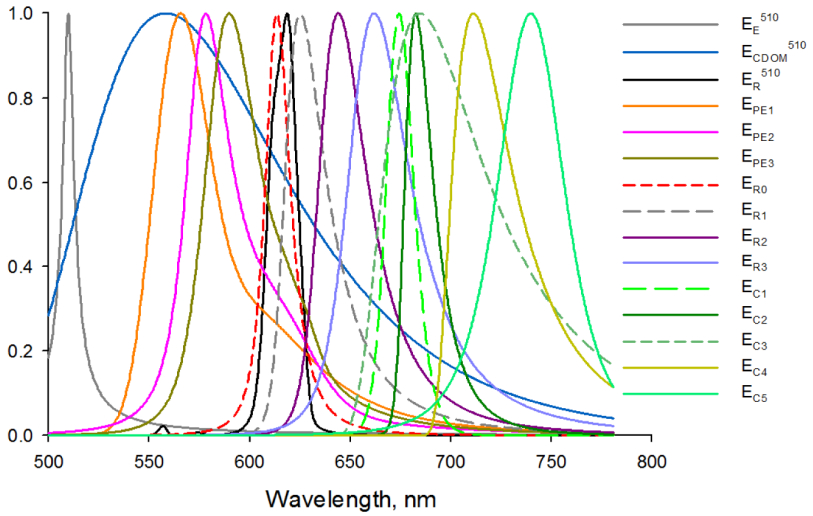

Fig. 4. A set of spectral components used for spectral deconvolution (SDC) of the LSE signatures of natural waters measured with laser excitation at 510 nm. See Tables 3 and 4 for detailed specification.

fluorescence do not depend on the excitation wavelength as long as it remains shorter than the pigment emission. The latter is valid for the 375, 405, 510, and 532 nm laser excitation used in various ALF instrument configurations (for example, see Fig. 4).

The extensive field measurements with the ALF instrument has resulted in refining the ALF SDC algorithms described in [9]. In particular, two additional Chl-a fluorescence components, $\mathbf{E_{C4}}$ and $\mathbf{E_{C5}}$ (fluorescence maxima at 711 and 740 nm, respectively) were added to extend the SDC analysis in the near-infrared spectral area mainly associated with Chl-a emission from photosystem I [60]. An additional red component, $\mathbf{E_{R0}}$ (λ_{max} = 613 nm), was also included to account for the red emission observed in the California Current and Gulf of Mexico. The red non-Chl-a fluorescence found in 405-nm-stimulated LSE field spectral measurements [9] still remains one of the most intriguing ALF findings, but it seems to be consistent with the independent recent detection of the ubiquitous dissolved pigment degradation product in subsurface waters of the global ocean [55].

The complete set of spectral components used for SDC analysis of ALF-T LSE spectral measurements include fifteen spectral components for each excitation wavelength (Table 3). The fluorescence spectra of organic molecules can be analytically described using the Pearson's IV function(s) [9]:

$$y = \frac{a_0\left[1+\frac{\left(x-\frac{a_2a_4}{2a_3}-a_1\right)^2}{a_2^{\,2}}\right]^{-a_3}\exp\left[-a_4\left(\tan^{-1}\left(\frac{x-\frac{a_2a_4}{2a_3}-a_1}{a_2}\right)+\tan^{-1}\left(\frac{a_4}{2a_3}\right)\right)\right]}{\left(1+\frac{a_4^{\,2}}{4a_3^{\,2}}\right)^{-a_3}} \quad (1)$$

Here, a_0, a_1, a_2, a_3, and a_4 are parameters that define respectively the amplitude, center, width, shape$_1$, and shape$_2$ of the fluorescence band; x is a wavelength (nm). A set of parameters that can be used for analytical description of the SDC components of fluorescence constituents and water Raman scattering is listed in Table 4 in the Appendix.

#189252 - $15.00 USD Received 23 Apr 2013; revised 23 May 2013; accepted 24 May 2013; published 7 Jun 2013

Table 3. SDC spectral components. For 405, 510, and 532 nm excitation, three bands of the water Raman scattering with the Raman shifts ν_{max} = 1660, 2200 and 3440 cm^{-1}, respectively, are integrated into one SDC component representing the Raman scattering in the LSE spectra. Spectral location of the individual Raman peak can be calculated as $\lambda_{max} = (\lambda_{exc}^{-1} - \nu_{max})^{-1}$; here, λ_{max} and λ_{exc} are the wavelengths of the Raman scattering peak and excitation, respectively. The grey-highlighted components do not contribute in the spectral range of ALF-T SDC analysis (>420 nm) and are not included in the SDC best fitting.

Component number	Spectral component	Abbreviation	Emission peak, nm
1^{375}	Elastic scattering	E_E^{375}	375
2^{375}	CDOM fluorescence	E_{CDOM}^{375}	472
3^{375}	Water Raman scattering, 1660, 2200, and 3440 cm^{-1}	E_R^{375}	400, 409, 431
1^{405}	Elastic scattering	E_E^{405}	405
2^{405}	CDOM fluorescence	E_{CDOM}^{405}	472
3^{405}	Water Raman scattering, 1660, 2200, 3440 cm^{-1}	E_R^{405}	434, 445, 471
1^{510}	Elastic scattering	E_E^{510}	509.8
2^{510}	CDOM fluorescence	E_{CDOM}^{510}	558
3^{510}	Water Raman scattering, 1660, 2200, 3440 cm^{-1}	E_R^{510}	557, 574, 619
1^{532}	Elastic scattering	E_E^{532}	532
2^{532}	CDOM fluorescence	E_{CDOM}^{532}	587
3^{532}	Water Raman scattering, 1660, 2200, 3440 cm^{-1}	E_R^{532}	583, 602, 651
4	Red emission 0	E_{R0}	613
5	Red emission 1	E_{R1}	625
6	Red emission 2	E_{R2}	644
7	Red emission 3	E_{R3}	662
8	PE fluorescence 1	E_{PE1}	565
9	PE fluorescence 2	E_{PE2}	578
10	PE fluorescence 3	E_{PE3}	589
11	Chl-a fluorescence 1	E_{C1}	674
12	Chl-a fluorescence 2	E_{C2}	683
13	Chl-a fluorescence 3	E_{C3}	685
14	Chl-a fluorescence 4	E_{C4}	711
15	Chl-a fluorescence 5	E_{C5}	740

In the ALF optical design, the LSE spectra are measured through long-pass filter or notch filter (depending on the instrument configuration) that reduces the intensity of elastic scattering of laser excitation. Nonetheless, the tale contribution of the excitation elastic scattering in the short-wavelength area of the SDC spectral range can be comparable to relatively weak fluorescence of the aquatic constituents and has to be accounted for in the SDC algorithm for correct fluorescence assessments. In the updated ALF-T SDC algorithms, the tale spectral distribution of elastic scattering of 510 nm laser excitation is approximated using Pearson's VII amplitude function:

$$y = \frac{a_0}{\left[1 + 4\left(\frac{x - a_1}{a_2}\right)^2 \left(2^{\frac{1}{a_3}} - 1\right)\right]^{a_3}} \quad (2)$$

Here, a_0, a_1, a_2, and a_3 are parameters that define respectively the amplitude, center, width, and shape of the spectral distribution; x is a wavelength (nm). The tale spectral contributions of 405 and 532 nm laser excitations are analytically approximated as described in [9]. The spectral contribution of elastic scattering of 375 nm laser excitation at wavelengths exceeding 420 nm, where the SDC is conducted, can be neglected as shown by our field tests. A

#189252 - $15.00 USD Received 23 Apr 2013; revised 23 May 2013; accepted 24 May 2013; published 7 Jun 2013

complete list of parameters describing the SDC spectral components listed in Table 3 is presented in Table 4 in the Appendix. A set of SDC components for analysis of LSE spectra of natural water stimulated with 510 nm laser is shown in Fig. 4.

5. Examples of ALF-T measurements

5.1 An example of ALF-T-510 measurements

The SDC analysis of ALF-T LSE spectral measurements and photo-physiological assessments of variable fluorescence from the ALF-T temporal measurements are conducted as described in [9]. Examples of the spectral and temporal LSE measurements in phytoplankton cultures of phycobiliprotein-containing *Rhodomonas sp.* (cryptophyte) and *Synechococcus spp.* (cyanobacteria) using the ALF-T-510 instrument configured with a flow-through sampling module are displayed in Fig. 5. Before the measurements, the samples were diluted with filtered seawater to concentration typical for estuarine waters. The LSE spectra (green dots in Figs. 5(a) and 5(c)) were measured over 1 s integration time and corrected for the instrument spectral response as described above. The golden solid lines represent best fitting with the SDC components listed in Table 3 and shown in Fig. 4. The spectral bands of laser elastic scattering (510 nm), CDOM fluorescence (560 nm), water Raman scattering (620 nm), cryptophyte-specific phycoerythrin fluorescence (590 nm), and Chl-a fluorescence (680 nm) provided the most significant contributions to the LSE spectrum of the sample containing *Rhodomonas sp.*. The phycoerythrin fluorescence typical for green-water cyanobacteria (peaking at 578 nm) and three red fluorescence bands of other PBP pigments (625, 644, 662 nm) are distinct features of the cyanobacterial spectral signature in Fig. 5(c). Note that the signal intensity in the spectral area of Chl-a fluorescence is formed by the overlap between CDOM, allophycocyanin, and Chl fluorescence (peaking at 558, 662, and 683 nm, respectively), and Chl-a fluorescence intensity is less than 50% of the total LSE intensity as a result of the significant non-Chl-a spectral background.

The LSE induction waveforms averaged over 25 shots are displayed with red dots in Figs. 5(b) and 5(d). The beginning of the laser excitation flash is marked "0" on the time scale. Both plots show gradual, almost exponential Chl-a fluorescence increase in LSE over 150 μs caused by the excitation-induced saturation of photosystem II photochemistry [23]. The blue lines in Figs. 5(b) and 5(d) show the magnitudes of non-chlorophyll fluorescence background calculated as described in [9] for each sample from the SDC analyses of the spectral measurement displayed in Figs. 5(a) and 5(c), respectively. Best fits with a bio-physical model [9] for assessments of photochemical efficiency, $\mathbf{F_v/F_m}$ ("variable fluorescence"), are displayed with white lines. After accounting for the non-chlorophyll fluorescence background the best fitting yielded $\mathbf{F_v/F_m}$ = 0.44 and $\mathbf{F_v/F_m}$ = 0.39 for the induction curves displayed in Figs. 5(b) and 5(d), indicating good functionality of photosynthetic apparatus for both phytoplankton samples. Note that calculating F_m from the zero base line, without subtracting the non-chlorophyll fluorescence background, would result in dramatic underestimation of F_v/F_m magnitude and the functional state of the cyanobacterial sample. Thus, neglecting the spectral complexity of aquatic fluorescence signatures may adversely affect the accuracy of fluorescence measurements and, in some cases, even result in misleading conclusions regarding phytoplankton photochemical functionality and photosynthetic performance. A number of publications (e.g [31,32,54,56–58,61].) report new observations and indicate growing understanding of this, and the ALF technique that uniquely combines spectral and temporal measurements may provide potential to address the issue.

#189252 - $15.00 USD Received 23 Apr 2013; revised 23 May 2013; accepted 24 May 2013; published 7 Jun 2013

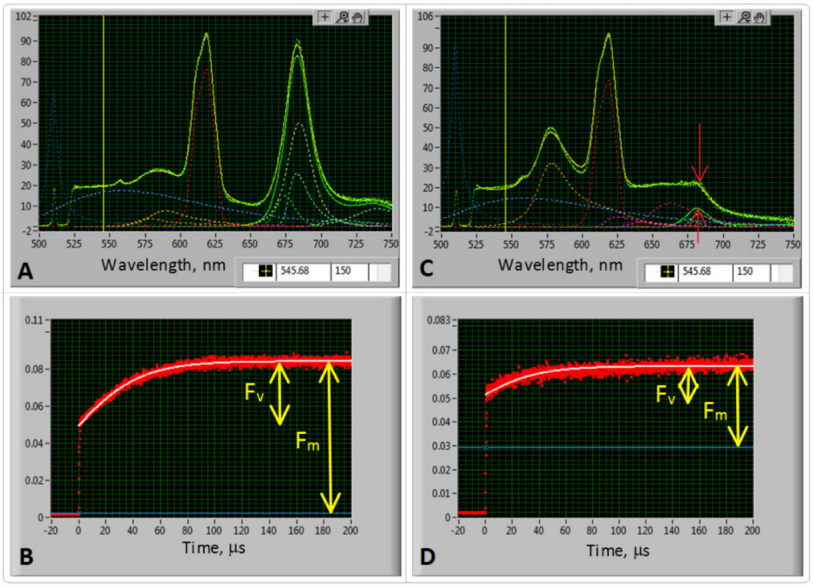

Fig. 5. Examples of ALF-T-510 spectral (upper) and temporal (lower) LSE measurements in samples of phytoplankton cultures *Rhodomonas Sp.* (cryptophytes) and *Synechococcus spp.* (cyanobacteria) diluted to naturally-occurring concentrations. **A, C:** The spectra (green dots) were corrected for the instrument spectral response. The SDC best fits with the scaled spectral components (dashed lines) are displayed with golden lines. **B, D:** The best fits to the measured LSE induction (red dots) with the biophysical model of Chl-a fluorescence induction [9] are displayed with white lines. Neglecting the non-chlorophyll spectral fluorescence background in the spectral area of Chl-a fluorescence (marked with red arrows in panel **C;** blue lines in panels (**B**) and (**D**) may result in significant underestimation of variable fluorescence, F_v/F_m.

5.2 An example of ALF-T-375/510/405 measurements

An example of spectrally and temporally resolved LSE measurement of a seawater sample with the ALF-T-375/405/510 instrument during a research cruise in the California Current (Aug. 2012) is displayed in Fig. 6. The spectra displayed in panels Figs. 6(a), 6(b), and 6(c) were measured with 405, 510, and 375 nm laser excitation, respectively, corrected for the instruments spectral response, and analyzed using the SDC algorithm with the spectral components displayed in Table 3 to assess the seawater fluorescent constituents. The water Raman scattering peaks are located at 470, 622, and 440 nm in Figs. 6(a), 6(b), and 6(c), respectively. The intense Chl-a fluorescence peaking at 680 nm indicates high Chl-a concentration. The broadband CDOM fluorescence was most efficiently stimulated with the UV excitation at 375 nm (Fig. 6(c)). Strong phycoerythrin fluorescence at 565 nm indicates significant abundance of blue-water cyanobacteria in the analyzed water (Fig. 6(b)). Relatively low fluorescence induction increase (Figs. 6(d) and 6(e)) suggests low photochemical efficiency and depressed photo-physiological state of phytoplankton.

An example of correlation between the independent fluorometric measurements of Chl-a concentration in pigment extracts and the SDC retrievals of Chl-a fluorescence normalized to water Raman scattering measured *in vivo* in seawater samples with ALF-T-375/405/510 instrument using 510 nm LSE excitation is displayed in Fig. 6(f). The high degree of correlation (R^2 = 0.94) illustrates the accuracy of ALF measurements and analytical algorithms.

#189252 - $15.00 USD Received 23 Apr 2013; revised 23 May 2013; accepted 24 May 2013; published 7 Jun 2013

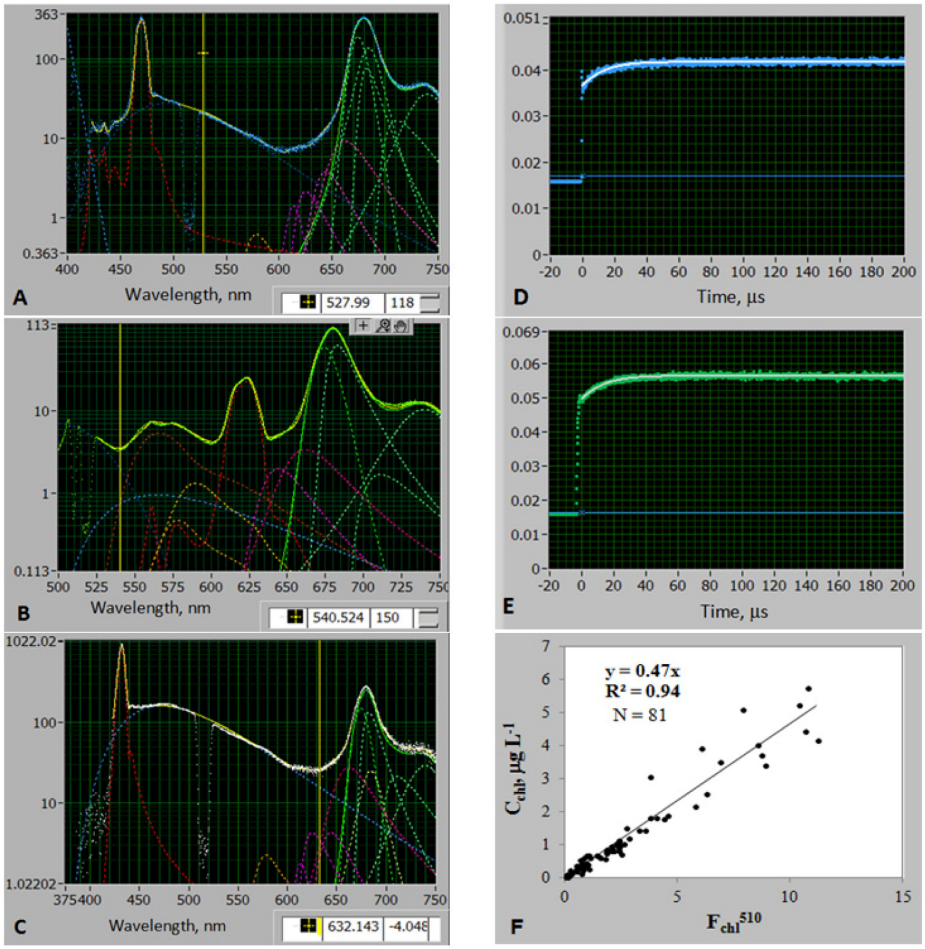

Fig. 6. An example of *in vivo* spectral (**A, B, C**) and temporal (**D, E**) LSE measurements in a seawater sample with the ALF-T-375/405/510 instrument (CCE LTER cruise, California Current, Aug. 2012). **A, D:** LSE excitation at 405 nm; **B, E:** LSE excitation at 510 nm; **C:** LSE excitation at 375 nm. Golden line in panels **A, B, C** displays the SDC best fit to the measured LSE spectra corrected to the instrument spectral response (blue, green and white dots in panels **A, B,** and (**C**), respectively; the SDC-scaled spectral components listed in Table 3 for each excitation wavelength are shown with dashed color lines). **D, E:** The best fit to the measured LSE induction (light blue and green dots in panels (**D**) and (**E**), respectively) with the biophysical model of Chl-a fluorescence induction [9] is displayed with white line. **F:** Correlation between Chl-a fluorescence normalized to water Raman scattering [9] measured *in vivo* in 81 seawater samples with ALF-T-375/405/510 instrument using 510 nm LSE excitation in diverse water types (CCE LTER cruise, California Current, Aug. 2012).

6. Conclusion

The next generation ALF technology has been developed for laboratory and field measurements on the basis of extensive field tests and deployments of the original ALF instrument. It uniquely combines spectral and temporal measurements of laser-stimulated sample emission for improved characterization of aquatic fluorescence constituents in natural waters. The new "T" optical design improves the efficiency of fluorescence excitation and collection and allows instrument configuration with one or several laser modules for fluorescence excitation. The instrument incorporates swappable sampling modules for flow-through analysis and discrete sample measurements, including small-volume samples in

#189252 - $15.00 USD Received 23 Apr 2013; revised 23 May 2013; accepted 24 May 2013; published 7 Jun 2013

standard 1x1x4 cm fluorometric cuvettes. The miniature peristaltic pump is used for sampling from 100 to 500 mL bottles. The basic single-laser instrument configuration, ALF-T-510, employs a new 510 nm laser and is capable of quite comprehensive characterization of aquatic fluorescence constituents, including Chl-a and phycobiliprotein pigments, variable fluorescence and CDOM in estuarine and fresh waters. The three-laser instrument configuration, ALF-T-375/405/510 provides additional UV and blue laser fluorescence excitation for measuring CDOM in diverse water types, phytoplankton photo-physiological assessments with dual-wavelength excitation, and potential for spectral discrimination between oil and CDOM fluorescence. The new ALF-T technology was successfully tested and deployed during the research cruise in the California Current. The results of the field studies will be reported in detail in the follow-up publications. The ALF-T technological development has resulted in the pending patent application. A commercial version of the next generation ALF instrument is currently under development in close collaboration with WET Labs, Inc., to provide new observational means for researchers and environmental monitoring. The *in situ* fiber-probe version of the ALF instrument, which is also part of this collaborative work, will further enhance our capacity for characterization of natural aquatic environments.

#189252 - $15.00 USD Received 23 Apr 2013; revised 23 May 2013; accepted 24 May 2013; published 7 Jun 2013

Appendix

Table 4. Parameters of Pearson's IV function for analytical approximation of SDC components listed in Table 3.

Compo-nent	Emission Band	λ_{max} nm	a_o	a_1	a_2	a_3	a_4
E_{CDOM}^{375}	CDOM fluorescence	472	1	471.7	3.77	5.75	–476
E_{CDOM}^{405}	CDOM fluorescence	492	1	492.2	9.91	6.81	–245
E_{CDOM}^{510}	CDOM fluorescence	558	1	558.3	11.4	5.70	–164
E_{CDOM}^{532}	CDOM fluorescence	581	1	581.1	6.85	1.66	–32.6
E_R^{375}	Raman scattering: 3440 cm^{-1}	431	1	432.1	9.40	5.95	4.35
			0.049	441.5	0.383	0.883	–14.9
E_R^{405}	Water Raman scattering: 1660, 2200, and 3440 cm^{-1}	471	0.025	422.3	1.49	0.413	–0.988
			0.016	434.8	1.35	0.789	0.540
			0.008	444.2	1.01	4.20	–76.5
			0.619	466.7	5.11	2.68	–0.539
			0.759	471.2	6.60	3.72	0.019
			0.190	474.8	3.62	4.54	12.3
			0.019	484.5	3.27	3.60	–23.3
E_R^{510}	Water Raman scattering: 1660, 2200, and 3440 cm^{-1}	619	0.0205	557.0	6.11	9.05	15.9
			0.00645	574.3	5.66	2.87	–0.455
			0.470	611.5	8.13	2.16	–1.81
			0.391	618.4	7.05	3.78	6.45
			0.398	622.6	9.19	3.81	6.73
E_R^{532}	Water Raman scattering: 1660, 2200, and 3440 cm^{-1}	651	0.042	583.3	2.24	0.852	0.650
			0.016	599.2	5.47	0.724	–0.710
			0.457	641.9	7.84	2.33	–0.291
			0.817	650.5	12.0	3.67	1.39
			0.169	657.9	2.87	3.35	19.6
			0.017	672.7	16.6	14.0	83.9
E_{R0}	Red emission 0	613	1	613.5	9.61	1.49	–0.517
E_{R1}	Red emission 1	625	1	625.1	12.1	1.59	–3.11
E_{R2}	Red emission 2	644	1	644.0	17.2	1.80	–2.63
E_{R3}	Red emission 3	662	1	661.9	23.0	1.62	–1.65
E_{C1}	Chl-a fl. 1	673	1	673.4	20.1	5.01	–2.81
E_{C2}	Chl-a fl. 2	683	1	682.6	9.60	2.12	–4.21
E_{C3}	Chl-a fl. 3	685	1	684.6	16.0	2.06	–0.168
E_{C4}	Chl-a fl. 4	711	1	711.2	9.14	2.02	–11.9
E_{C5}	Chl-a fl. 5	740	1	739.8	33.3	2.33	0.0291
E_{PE1}	PE fluorescence 1	565	0.985	565.4	58.1	12.3	–16.9
			0.233	610.9	35.3	1.85	–2.49
E_{PE2}	PE fluorescence 2	578	0.954	577.9	14.1	1.14	–0.78
			0.163	613.8	70.3	8.17	7.74
E_{PE3}	PE fluorescence 3	590	1.000	589.8	21.0	1.56	–1.40
			0.056	617.1	14.6	3.57	–1.59
			0.063	628.1	18.1	4.67	0.487
E_E^{375}	Elastic scattering	375	-	-	-	-	-
E_E^{405}	Elastic scattering, $y = a_0 \exp(-a_1\lambda)$	405	6.85^{30}	1.68^{-1}	-	-	-
E_E^{510}	Elast. Scat. (Eq. (2))	510	1	509.8	7.69	0.655	-
E_E^{532}	Elastic scattering	532	1	543.9	0.913	1.01	–15.7

Acknowledgments

This work was sponsored by the NOPP program (Award # N000141010205). We thank Dr. Juhl for phytoplankton cultures, the California Current Ecosystem Long Term Ecological Research program for the field opportunity, and Ralf Goericke and Megan Roadman for their chlorophyll data. Our special thanks to the captain, crew, and resident technicians of the R/V *Melville* on the CCE LTER cruise. We would like to thank two anonymous reviewers for their useful comments and suggestions that helped to improve the manuscript.